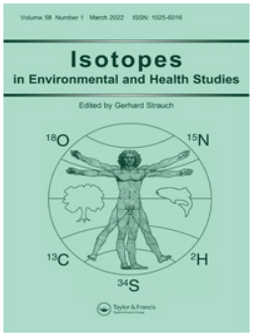

Isotopes in Environmental and Health Studies

ISSN: (Print) (Online) Journal homepage: https://www.tandfonline.com/loi/gieh20

Quantifying the contribution of evaporation from Lake Taihu to precipitation with an isotope-based method

Yongbo Hu, Wei Xiao, Jingyuan Wang, Lisa R. Welp, Chengyu Xie, Haoran Chu & Xuhui Lee

To cite this article: Yongbo Hu, Wei Xiao, Jingyuan Wang, Lisa R. Welp, Chengyu Xie, Haoran Chu & Xuhui Lee (2022): Quantifying the contribution of evaporation from Lake Taihu to precipitation with an isotope-based method, Isotopes in Environmental and Health Studies, DOI: 10.1080/10256016.2022.2056599

To link to this article: https://doi.org/10.1080/10256016.2022.2056599

Published online: 05 Apr 2022.

Submit your article to this journal

View related articles

View Crossmark data

Full Terms & Conditions of access and use can be found at
https://www.tandfonline.com/action/journalInformation?journalCode=gieh20

ISOTOPES IN ENVIRONMENTAL AND HEALTH STUDIES
https://doi.org/10.1080/10256016.2022.2056599

Taylor & Francis
Taylor & Francis Group

Check for updates

Quantifying the contribution of evaporation from Lake Taihu to precipitation with an isotope-based method

Yongbo Hu [a], Wei Xiao [a], Jingyuan Wang [b], Lisa R. Welp [c], Chengyu Xie [a], Haoran Chu [a] and Xuhui Lee [d]

[a]Yale-NUIST Center on Atmospheric Environment, International Joint Laboratory on Climate and Environment Change (ILCEC), Nanjing University of Information Science and Technology, Nanjing, People's Republic of China; [b]Key Laboratory of Ecosystem Network Observation and Modeling, Institute of Geographic Sciences and Natural Resources Research, Chinese Academy of Sciences, Beijing, People's Republic of China; [c]Department of Earth, Atmospheric, and Planetary Sciences, Purdue University, West Lafayette, IN, USA; [d]School of the Environment, Yale University, New Haven, CT, USA

ABSTRACT

Moisture recycling plays a crucial role in regional hydrological budgets. The isotopic composition of precipitation has long been considered as a good tracer to investigate moisture recycling. This study quantifies the moisture recycling fractions (f_r) in the Lake Taihu region using spatial variations of deuterium excess in precipitation (d_P) and surface water vapour flux (d_E). Results show that d_P at a site downwind of the lake was higher than that at an upwind site, indicating the influence of lake moisture recycling. Spatial variations in d_P after sub-cloud evaporation corrections were 2.3, 1.4 and 3.2 ‰, and d_E values were 27.4, 32.3 and 31.4 ‰ for the first winter monsoon, the summer monsoon and the second winter monsoon, respectively. Moisture recycling fractions were 0.48 ± 0.13, 0.07 ± 0.03 and 0.38 ± 0.05 for the three monsoon periods, respectively. Both using the lake parameterization kinetic fractionation factors or neglecting sub-cloud evaporation would decrease f_r, and the former has a larger influence on the f_r calculation. The larger f_r in the winter monsoon periods was mainly caused by lower specific humidity of airmasses but comparable moisture uptake along their trajectories compared to the summer monsoon period.

ARTICLE HISTORY
Received 20 August 2021
Accepted 5 March 2022

KEYWORDS
China; evaporation; hydrogen-2; lake; modelling; moisture; monsoon; oxygen-18; recycling; water

1. Introduction

Contribution of lake evaporation to precipitation, referred to as moisture recycling, is an important source of downwind precipitation [1–4]. In temperate climates, it can account for as much as 50% of precipitation [2]. Accurate quantification of moisture recycling can improve our understanding of surface–air interactions [5,6] and can serve as a powerful validation of atmospheric water budget predictions from regional climate models [7,8].

Up to now, most of the lake water recycling studies have been conducted for temperate [1–4,9–11] and plateau climate regions [3]. Our knowledge is relatively poor about water recycling in tropical and subtropical climates. About 13% of inland lakes are

CONTACT Wei Xiao wei.xiao@nuist.edu.cn; Jingyuan Wang wangjy@igsnrr.ac.cn
© 2022 Informa UK Limited, trading as Taylor & Francis Group

located in these zones, occupying a total area of $4.35 \cdot 10^5$ km^2 [12]. Their impacts on local climate are different from mid- to high-latitude lakes. For example, at Lake Taihu (also called Lake Tai, but Lake Taihu is more commonly used), a subtropical lake in the Yangtze River Delta (YRD), China, located between 30.0944°N and 31.5494°N in latitude and 119.8755°E and 120.6028°E in longitude, the lake–land breeze circulation is much weaker than that associated with the Great Lakes of North America, owing to a weaker lake–land thermal contrast which was caused by the shallower lake depth [13]. On the other hand, the lake–land Bowen ratio contrast is larger at Lake Taihu than at Lake Superior [14,15], implying a larger contribution of lake evaporation to the regional water cycle.

Atmospheric models [16–18], back-trajectory analysis [11,19,20] and isotope-based methods [1,4,21,22] are three most commonly used methods to quantify the moisture recycling. In atmospheric modeling studies, the recycling fraction is computed as the ratio of water evaporated from the surface and that transported from outside the local atmospheric domain. In trajectory analysis, the effect of surface evaporation on the airmass is reflected via increase of specific humidity which counteracts the decrease due to precipitation. Isotope-based methods make use of the unique physical characteristics of different water isotopologues to quantify the moisture recycling. Compared with the other two methods, one of the biggest advantages of the isotope-based methods is that water vapour isotopic compositions are natural integrators of advection effect and local effects [23,24], especially for deuterium excess (*d*-excess), which unlike ^{2}H and ^{18}O would not be influenced by the equilibrium fractionation process, thus requiring relatively few observation sites. However, uncertain kinetic fractionation associated with lake evaporation and sub-cloud evaporation can complicate the interpretation of these effects [9,10,25,26]. Typically, the isotopic composition of evaporation is determined with the Craig–Gordon model [27]. Recent studies have shown that this model is sensitive to the selection of the kinetic fractionation factor for open water evaporation [28–30]. Xiao et al. [26] reported that if a commonly used kinetic factor of lake parameterization is used, the recycling fraction is 0.07 for the Great Lakes, but this recycling fraction is changed to 0.17 if the fractionation factor of oceanic parameterization which has been validated by Xiao et al. [29] at Lake Taihu is used instead. As raindrops descend from the saturated cloud layer to the unsaturated sub-cloud atmospheric layer, they will undergo evaporation, a process that will reduce their *d*-excess [31–34]. If this sub-cloud kinetic fractionation effect is not properly accounted for, moisture recycling fraction would be biased low [25]. The accurate way to constrain both is important to quantify the moisture recycling fraction.

Previous studies have shown that f_r can vary seasonally due to evaporation seasonality [4,11,16,35,36] and changes in moisture source regions [18,37,38]. In the YRD, lake evaporation during the summer monsoon period (June to September) is five times as large as that during the winter monsoon period (December to February) [14,39,40]. Additionally, in the summer, abundant atmospheric moisture is transported from South China Sea and East China Sea, whereas in the winter the source of moisture is the continental landmass to the north and northwest and is much weaker [41,42]. A reasonable hypothesis is that moisture recycling in the Lake Taihu region is stronger in the winter than in the summer because the lake evaporation contributes relatively more to a smaller monsoon atmospheric moisture background.

In this study, we quantify the contribution of evaporation from Lake Taihu to precipitation at a station downwind of the lake. Key to our methodology is a two-component mixing model driven by simultaneous measurements of precipitation isotopic compositions around the lake and water vapour isotopic compositions over the lake.

Our specific aims are (1) to quantify the moisture recycling fraction for this subtropical lake; (2) to evaluate the sensitivity of the two-component model to the kinetic effects of surface evaporation and raindrop evaporation; and (3) to investigate seasonal variability of the recycling fraction and the underlying mechanisms.

2. Materials and methods

2.1. Study area

Lake Taihu, with an area of approximately 2400 km^2 and a mean depth of 1.9 m, is located in the YRD in Eastern China (Figure 1). The study area has a typical humid subtropical monsoon climate. The prevailing wind direction is southeasterly during the summer monsoon and northerly during the winter monsoon. The annual air mean temperature from 1991 to 2020 was 16.8 °C, and annual precipitation was 1184 mm, with 650 and 160 mm during the summer and winter monsoon seasons, respectively. The annual evaporation of Lake Taihu from 2011 to 2017 was 1045 mm [40], which is comparable to annual precipitation. About 440 and 74 mm of evaporation occurred during the summer and winter monsoon seasons, respectively [40].

2.2. Data

2.2.1. Isotopic compositions of precipitation and lake water

Precipitation samples were collected at the Liyang (31.43°N, 119.48°E) and Dongshan (31.07°N, 120.43°E) stations from September 2015 to March 2017. Rain gauges with a 20-cm diameter (collecting area $3.14 \cdot 10^{-4}$ m^2) were modified to collect precipitation samples. Placed on top of these rain gages were funnels with a ping-pong ball at the

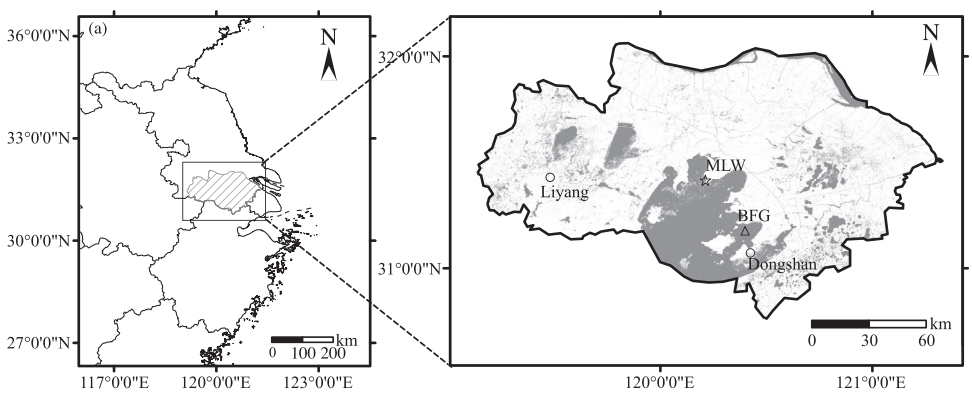

Figure 1. Map of Lake Taihu watershed, precipitation sampling sites (circles), site of water vapour and lake water isotope observation (star), and eddy-covariance site (triangle). Gray colour in panel b indicate water surface land covers (http://data.ess.tsinghua.edu.cn).

neck [43,44]. During a rain event, the ball would float, allowing rainwater to enter the gage. During non-raining periods, the ball would rest on the funnel's opening thus preventing the collected water from evaporating. Precipitation samples were collected after each event if it was shorter and did not pass 08:00 or 20:00 Beijing standard time. Otherwise, samples were additionally collected at 08:00 or 20:00. A total of 190 precipitation samples were collected at the Liyang station, and 211 at the Dongshan station. Lake water samples were collected at the Meiliangwan site (MLW, 31.4197°N, 120.2139°E, Figure 1) of the Taihu Eddy Flux Network [45], located in the northern part of Lake Taihu, 200 m away from the northern shore. The lake water at 20 cm depth were collected at 13:00 every day.

Water samples were stored in glass bottles, sealed with parafilm and placed in refrigerators with temperature of 4 °C to prevent evaporation. The H^2HO and $H_2^{18}O$ compositions of the precipitation and lake water samples were analysed using an isotope ratio infrared spectroscopy (IRIS) liquid water isotope analyser (Model DLT-100; Los Gatos Research, Mountain View, CA, USA) in the Key Laboratory of Ecosystem Network Observation and Modeling, Chinese Academy of Science. Each sample was measured 6 times, and the first two values were discarded to avoid the memory effect of the analyser [46]. The H^2HO and $H_2^{18}O$ compositions were expressed using the δ notation in reference to the Vienna Standard Mean Ocean Water (VSMOW). The precision of the analyser was 0.3 and 0.1 ‰ for δ^2H and $\delta^{18}O$, respectively. The isotope analyser was calibrated with working standards traceable to primary standards (VSMOW and Standard Light Antarctic Precipitation) distributed by the International Atomic Energy Agency.

2.2.2. Isotopic composition of water vapour

The measurement of water vapour isotopic composition was conducted at the MLW site from June 2012 to March 2017, covering the precipitation isotope sampling period. The raw data measured at 2 Hz were averaged to hourly intervals. The water vapour concentration and the isotopic compositions (H^2HO and $H_2^{18}O$) were measured at 3.5 m height above the water surface with a continuous IRIS analyser (Model 911-0004; Los Gatos Research, Mountain View, CA, USA). The linear distance of this analyser from the northern shore was 250 m. The 2-min precision was 0.2 ‰ for $\delta^{18}O_V$ and 2 ‰ for δ^2H_V, respectively [29]. Hourly data gaps in $\delta^{18}O_V$ and δ^2H_V were filled with a logarithmic relationship between $\delta^{18}O_V$ or δ^2H_V and specific humidity. Other details of this experiment can be found in Xiao et al. [29].

2.2.3. Meteorological and flux data

Hourly data on temperature, precipitation, air pressure, relative humidity, wind speed and wind direction were obtained from the two precipitation sampling sites, i.e. Liyang Meteorological Station and Dongshan Meteorological Station. At the MLW site, temperature and relative humidity were measured using an air temperature and humidity sensor (Model HMP45C, Vaisala Inc., Helsinki, Finland), and wind speed and direction were measured with an anemometer and wind vane (Model 03002, RM Young Company, Traverse City, MI, USA). These meteorological parameters were measured at 3.5 m height above the lake surface on a half-hourly scale.

Monthly mean lake surface temperature and monthly total lake evaporation was summarized from observations at the Bifenggang (BFG) site of the Taihu Eddy Flux Network. The surface temperature was inverted from the outgoing longwave radiation using the

Stefan–Boltzmann law [13,47,48]. These measurements were used to represent the whole-lake conditions due to little spatial variations of lake surface temperature, net radiation and latent heat flux across the lake [13]. Data gaps shorter than 1 h were filled by linear interpolation. Longer gaps were filled with linear regression against observations at a nearby lake site in the case of outgoing longwave radiation and with the bulk transfer method in the case of lake evaporation [48].

2.3. Two-component mixing model

A two-component mixing model [21] was used to quantify the recycled moisture fraction for the Lake Taihu region. The underlying assumption is that precipitation is a mixture of vapour advected from outside the local domain and vapour evaporated from local sources [21,25,49]. The two-source model expresses the recycling fraction f_r as

$$f_r = \frac{d_{down} - d_{adv}}{d_E - d_{adv}} \tag{1}$$

where d_E is the d-excess of the lake surface water vapour flux, calculated using the Craig–Gordon model (details in Section 2.5), and d_{down} and d_{adv} are the d-excess of water vapour (d_{PV}) at cloud base at the downwind site and upwind site, respectively. d_{PV} was assumed to be equilibrium with the condensed precipitation at cloud base which can be corrected from the observed d_P (details in Section 2.4).

The prevailing wind direction was southeasterly during the summer monsoon seasons (from June to September) and northerly during the winter monsoon seasons (from December to February). The Dongshan site was chosen as the upwind site and the Liyang site as the downwind site for the summer monsoon period *vice versa* for the winter monsoon period. The whole study period consisted of two winter monsoons (from December 2015 to February 2016 and from December 2016 to February 2017) and one summer monsoon (from June to September 2016).

2.4. Sub-cloud evaporation calibration

The sub-cloud evaporation effect is given as the difference of d-excess in precipitation between the ground and the cloud base ($\Delta d = d_P - d_{PV}$) and is calculated from

$$\Delta d = \Delta\delta^2\mathrm{H} - 8\Delta\delta^{18}\mathrm{O} \tag{2}$$

Here the parameters $\Delta\delta^2$H and Δδ18O represent the difference in $\delta^2\mathrm{H}_P$ and $\delta^{18}\mathrm{O}_P$ between the ground and the cloud base, and can be expressed as [25]:

$$\Delta\delta = \left(1 - \frac{\gamma}{\alpha_{eq}}\right)(f^{\beta} - 1) \tag{3}$$

where parameters γ and β can be calculated with the following equations [50]:

$$\gamma = \frac{\alpha_{eq} h}{1 - \alpha_{eq}(D/D')^k(1-h)} \tag{4}$$

$$\beta = \frac{1 - \alpha_{eq}(D/D')^k(1-h)}{\alpha_{eq}(D/D')^k(1-h)} \tag{5}$$

where the equilibrium fractionation factor α_{eq} was calculated as a function of condensation temperature T_{LCL} [51], T_{LCL} is determined with the 1.5 m air temperature T and dew point temperature T_d [52]:

$$T_{LCL} = T_d - (0.001296T_d + 0.1936)(T - T_d) \tag{6}$$

h is the 1.5-m relative humidity in fraction, D and D' are the molecular diffusion coefficients of the lighter ($H_2^{16}O$) and heavier isotopes (H^2HO or $H_2^{18}O$), and k is a parameter related to raindrop size and set to be 0.58 [50]. The mass fraction of the raindrop that reaches the ground, f, is given by:

$$f = \frac{m_{end}}{m_{end} + Et} \tag{7}$$

where the mass of the raindrop that reaches the ground m_{end} was calculated as a function of the radius of the raindrop (r), assuming the shape of the raindrop is sphere. The raindrop radius r (mm) can be obtained from an empirical formula [53]:

$$r = \frac{1}{2}\sqrt[c]{0.69}AI^q \tag{8}$$

where I is the precipitation intensity (in mm hour^{-1}), and the empirical coefficients c, A and q are 2.25, 1.30 and 0.232, respectively.

E is the evaporation rate of the raindrop determined by T, r and h [25,49],

$$E = Q_1 \times Q_2 \tag{9}$$

where

$$Q_1 = (-0.2445T + 131.28) \times (0.2r)^{1.6139} \tag{10}$$

$$Q_2 = (-0.73h + 0.7264) \times e^{(-0.002h+0.0371)T} \tag{11}$$

and the falling time of the raindrop t was determined with the height of the cloud base (H) and the falling velocity (v). The height of the cloud base is calculated as [54]:

$$H = 18400 \times \left(1 + \frac{T_{ave}}{273}\right)\log\frac{P_0}{P_{LCL}} \tag{12}$$

where P_0 is the surface atmospheric pressure, T_{ave} is the mean air temperature, and P_{LCL} is the atmospheric pressure at the height of the cloud base and can be expressed as [52]:

$$P_{LCL} = P_0\left(\frac{T_{LCL}}{T}\right)^{3.5} \tag{13}$$

v can be determined by H and r [55]:

$$v = \begin{array}{c} 9.58e^{0.035H}[1 - e^{-(r/1.77)^{1.147}}]\ (0.3 < r < 6) \\ 1.88e^{0.0256H}[1 - e^{-(r/0.304)^{1.819}}]\ (0.05 < r < 0.3) \\ 28.40r^2e^{0.0172H}\ (r < 0.05) \end{array} \tag{14}$$

After obtaining the corrected coefficient Δd, d_{PV} can be expressed as

$$d_{PV} = d_P - \Delta d \tag{15}$$

2.5. The Craig–Gordon model

The Craig–Gordon model was used to estimate the isotopic composition of lake evaporation (δ_E). The model expresses δ_E (in ‰) as [56]:

$$\delta_E = \frac{\alpha_{eq}^{-1}\delta_L - h\delta_v - \varepsilon_{eq} - (1-h)\varepsilon_k}{1 - h + 10^{-3}(1-h)\varepsilon_k} \tag{16}$$

where the equilibrium fractionation factor α_{eq} was calculated as a function of water surface temperature [51], ε_{eq} (in ‰) is given by $\varepsilon_{eq} = 10^3(1 - 1/\alpha_{eq})$, δ_L is the isotopic composition of the lake water (in ‰), h is relative humidity (in fraction) in reference to the water surface temperature, and ε_k is isotopic kinetic fractionation factor (in ‰), which was calculated with the wind-dependent parameterization of Merlivat and Jouzel [57]. This parameterization was independently validated at Lake Taihu [29]. In this study, δ_E was calculated on the monthly scale. Seasonal δ_E was calculated from monthly δ_E weighted by the monthly lake evaporation. The *d*-excess of lake evaporation, d_E was calculated from the δ_E of $H_2^{18}O$ and the δ_E of H^2HO.

2.6. Water transport trajectories

The Hybrid Single-Particle Lagrangian Integrated Trajectory (HYSPLIT) model was used to investigate the moisture source of precipitation and modification of the airmass by surface evaporation along its transport trajectories [58–61]. The atmospheric wind and moisture data from the Global Data Assimilation System (GDAS, ftp://arlftp.arlhq.noaa.gov/pub/archives/gdas1), with a 1°×1° grid resolution and 23 pressure layers, were used to compute the back trajectories 4 times a day, at 02:00, 08:00, 14:00 and 20:00 local time, at a receptor height of 1500 m above the mean sea level, over the precipitation collection stations, during rainy days. These trajectories consisted of consecutive vectors each representing the spatial displacement of the air parcel over one integration time step. The back trajectories ended at the grid cell that contained the precipitation measurement station. If the change in specific humidity for a grid cell increases by more than 0.2 g kg^{-1}, it is considered that the moisture is supplemented by surface evaporation at that time and location [58].

3. Results

3.1. The isotopic composition in precipitation

The temporal variation of monthly precipitation is presented in Figure 2. The monthly precipitation varied from 20 to 530 mm at Liyang station and from 13 to 339 mm at Dongshan station. The seasonal variation of precipitation was similar between Liyang and Dongshan stations. During the observation period, there were two precipitation peaks. The first peak occurred in June 2016, the beginning of the summer monsoon and the second peak appeared at the end of the summer monsoon (September or October 2016). The minimum occurred in August 2016.

The monthly amount-weighted δ^2H_P, $\delta^{18}O_P$ and d_P at Liyang and Dongshan stations are shown in Figure 2. The δ^2H_P ranged from −100.5–2.4 ‰ at Liyang station and from −76.6 to −8.8 ‰ at Dongshan station. For $\delta^{18}O_P$, the values ranged from −14.2 to

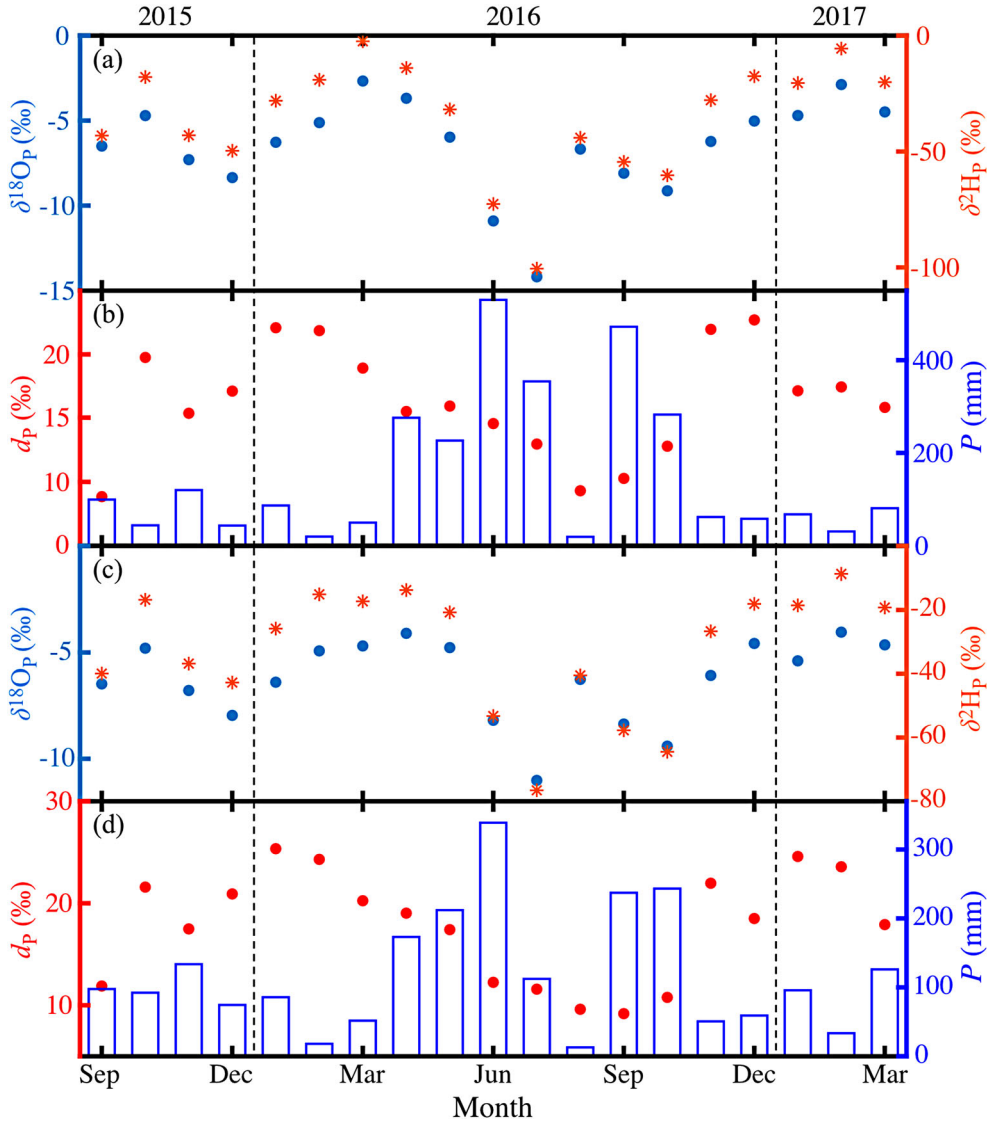

Figure 2. Time series of monthly amount-weighted δ^2H_P, $\delta^{18}O_P$ and d_P and precipitation at the Liyang (a and b) and Dongshan stations (c and d) from September 2015 to March 2017. The dashed lines represent the end of 2015 and 2016, respectively.

−2.7 ‰ at Liyang station and from −11.0 to −4.0 ‰ at Dongshan station. The d_P values varied from 8.8–22.7 ‰ at Liyang station and from 9.2–25.3 ‰ at Dongshan station. Temporal variations of δ^2H_P and $\delta^{18}O_P$ at the two sites showed similar patterns, with δ^2H_P and $\delta^{18}O_P$ more enriched in the winter and spring and more depleted in the summer. The d_P was lower in summer, at about 10 ‰, and higher in the winter and spring, at about 20 ‰.

The spatial variations of δ^2H_P, $\delta^{18}O_P$ and d_P are shown in Table 1. δ^2H_P and $\delta^{18}O_P$ at the downwind site were lower than those at the upwind site except the δ^2H_P in the first winter monsoon. The spatial variations (downwind minus upwind) were larger in

Table 1. Amount-weighted observed δ^2H_P, $\delta^{18}O_P$ and d_P and the corresponding values after sub-cloud evaporation correction (given in parentheses) at the Liyang and Dongshan station during the three monsoon periods.

Sites	Parameters	WM1	SM	WM2
Liyang	δ^2H_P (‰)	−33.2* (−35.7)*	−73.2 (−74.1)	−16.4* (−17.7)*
	$\delta^{18}O_P$ (‰)	−6.7* (−7.3)*	−10.7 (−11.0)	−4.5* (−4.9)*
	d_P (‰)	20.4* (22.7)*	12.4 (13.9)	19.6* (21.5)*
Dongshan	δ^2H_P (‰)	−31.8 (−33.4)	−58.3* (−59.5)*	−16.7 (−18.5)
	$\delta^{18}O_P$ (‰)	−6.9 (−7.3)	−8.7* (−9.0)*	−4.9 (−5.4)
	d_P (‰)	23.4 (25.0)	11.3* (12.5)*	22.5 (24.7)

Notes: WM1 represents the first winter monsoon period (from December 2015 to February 2016); SM represents summer monsoon period (from June to September 2016); WM2 represents the second winter monsoon period (from December 2016 to February 2017). The superscript * indicates value of the upwind site.

magnitude in the summer monsoon period, with values of −14.9 and −2.0 ‰ for δ^2H_P and $\delta^{18}O_P$, respectively, than in the winter monsoon periods, with values of 1.4 and −0.2 ‰ for δ^2H_P and $\delta^{18}O_P$ in the first winter monsoon period, respectively, and −0.3 and −0.4 ‰ for δ^2H_P and $\delta^{18}O_P$ in the second winter monsoon period, respectively. The d_P at the downwind site was greater than at the upwind site in all seasons. This spatial variation of d_P was lower in the summer monsoon period than in the winter monsoon periods: the difference (downwind minus upwind) was 3.0, 1.1 and 2.9 ‰ for the first winter monsoon period, the summer monsoon period, and the second winter monsoon period, respectively.

The influence of sub-cloud evaporation on remaining raindrops fraction (f) and isotopic compositions of precipitation are shown in Figure 3 and Table 1. On monthly scale, f varied from 88 to 99% at Liyang station and from 80 to 99% at Dongshan station. $\Delta\delta^2H$ ranged from 1.3–8.3 ‰ at Liyang station and from 1.2–6.9 ‰ at Dongshan station. $\Delta\delta^{18}O$ ranged from 0.3–2.1 ‰ at Liyang station and from 0.3–2.0 ‰ at Dongshan station. Δd varied from −8.1 to −1.4 ‰ at Liyang station and from −9.0 to −1.3 ‰ at Dongshan station. Generally speaking, the effects of sub-cloud evaporation on isotopic compositions of precipitation were comparable between the two sites, and no obvious seasonal pattern was observed. After correction for sub-cloud evaporation, the spatial variation in d_P (downwind minus upwind) was 2.3, 1.4 and 3.2 ‰ for the three monsoon periods, respectively.

3.2. Isotopic compositions of lake water, water vapour and evaporation

The kinetic fractionation factors were key parameters in the Craig–Gordon model to simulate the isotopic compositions of evaporation. They were determined by wind speed according to the oceanic parameterization of Merlivat and Jouzel [57]. In [57], the kinetic factors are implicit functions of wind speed. Here we used the polynomial functions provided by Xiao et al. [29] which are the best fit to the original parameterization. At the MLW site, the maximum monthly wind speed (3.1 m s^{-1}) occurred in April 2016, and the corresponding kinetic fractionation factors were 6.86 and 6.05 ‰ for ^{18}O and

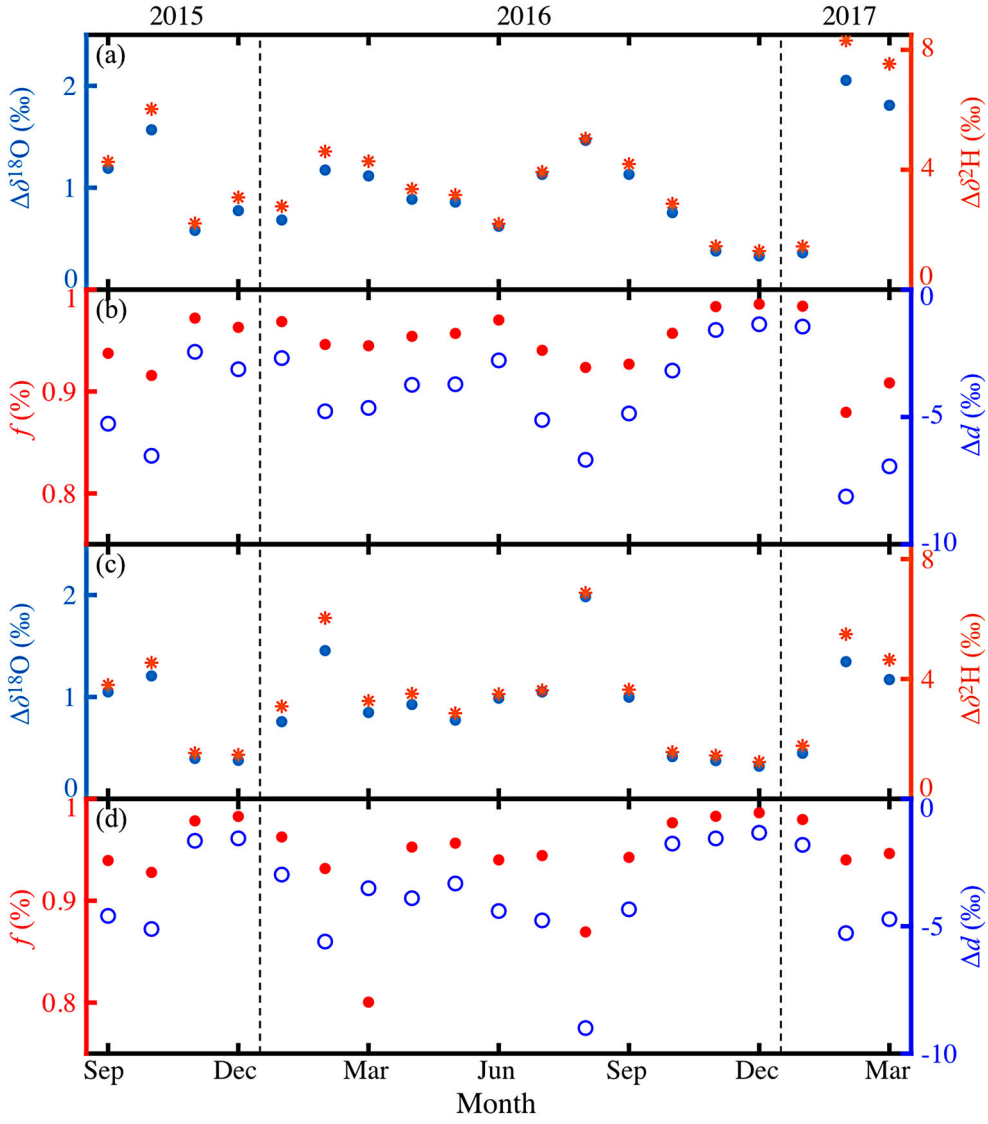

Figure 3. Influence of sub-cloud evaporation on remaining raindrop fraction (f) and isotopic compositions of precipitation. $\Delta\delta^2$H, $\Delta\delta^{18}$O and Δd are differences in δ^2H, δ^{18}O and d between the ground and the cloud base. Panels a and b: Liyang; panels c and d: Dongshan. The dashed lines represent the end of 2015 and 2016, respectively.

^{2}H, respectively (Figure 4(a)). The minimum wind speed (2.0 m s^{-1}) appeared in November 2016, and the corresponding kinetic fractionation factors were 7.29 and 6.43 ‰ for ^{18}O and ^{2}H, respectively.

The isotopic compositions of lake surface water (δ^2H_L and $\delta^{18}O_L$) and water vapour (δ^2H_V and $\delta^{18}O_V$), two input variables of the Craig–Gordon model, are shown in Figure 4. During the observation period, monthly δ^2H_L ranged from −47.4 to −25.0 ‰, and monthly $\delta^{18}O_L$ varied from −6.9 to −3.8 ‰. Large temporal variations of δ^2H_L and $\delta^{18}O_L$ were observed, with the maximum occurring in May 2016 and the minimum

occurring in December 2016. The d_L ranged from −2.1–8.6 ‰, with lower values in the summer and early autumn and larger values in the winter and spring. The monthly δ^2H_V ranged from −126.7 to −98.9 ‰. The monthly $\delta^{18}O_V$ varied from −19.6 to −15.0 ‰. The range of d_V was from 17.0 ‰ to 30.2 ‰, without an obvious seasonal pattern.

The monthly isotopic compositions of evaporation are also shown in Figure 4. The δ^2H_E varied from −174.7 to −74.1 ‰, and $\delta^{18}O_E$ ranged from −26.5 to −13.2 ‰. The seasonality was similar in δ^2H_E and $\delta^{18}O_E$, with less negative values in the summer and more negative values in the winter. The d_E was always positive without an obvious seasonality,

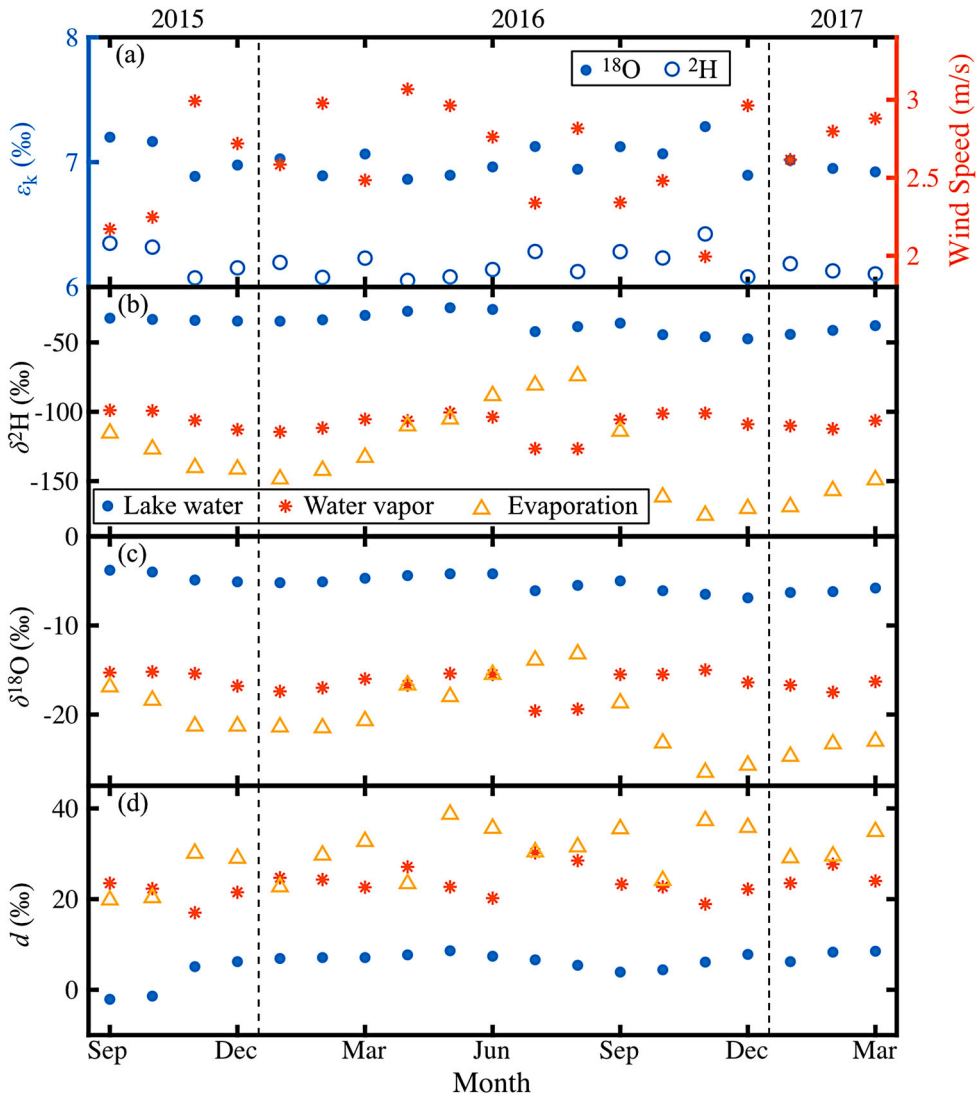

Figure 4. The monthly averaged isotope input parameters of the Craig–Gordon model, i.e. kinetic fractionation factors determined with wind speed, isotopic compositions of lake water and water vapour observed at MLW site, and output parameters, i.e. isotopic compositions in evaporation. The dashed lines represent the end of 2015 and 2016, respectively.

ranging from 19.8–38.7 ‰. Weighted by the monthly evaporation, the d_E was 27.4, 32.3 and 31.4 ‰ for the first winter monsoon period, the summer monsoon period and the second winter monsoon period, respectively.

3.3. Moisture recycling fraction

The moisture recycling fraction at Lake Taihu region, determined with the two-component mixing model (Equation (1)), was 0.48 ± 0.13 (mean ± 1 standard deviation), 0.07 ± 0.03 and 0.38 ± 0.05 for the first winter monsoon, the summer monsoon and the second winter monsoon, respectively (Table 2). The recycling fraction f_r was about 4–6 times larger in the winter monsoon than in the summer monsoon. The standard deviation of f_r was obtained by a Monte Carlo simulation, using uncertainties in d_{PV} of 1.1 ‰ and d_E of 2.1 ‰.

3.4. Back trajectories analyses

The back trajectories simulated with the HYSPLIT model show different patterns of humidity transport during the summer and the winter monsoon periods (Figure 5). During the summer monsoon period, moisture mostly derived from the South China Sea and the Western Pacific Ocean was associated with high specific humidity (12–20 g kg^{-1}). In contrast, during the winter monsoon periods when the moisture source turned to the inland, specific humidity along the winter transport trajectories was much lower, varying from 0 to 8 g kg^{-1}. However, moisture uptake was similar between the summer monsoon period and the winter monsoon periods, mostly below 2 g kg^{-1} over the duration of the trajectory simulation (Figure 6).

4. Discussion

4.1. Influence of kinetic processes on the calculation of moisture recycling fraction

The moisture recycling fraction from the two-source model is sensitive to the kinetic processes associated with surface evaporation and sub-cloud evaporation [25,26]. The isotopic composition of lake evaporation is sensitive to the parameterization of kinetic fractionation [29]. Errors due to inaccurate kinetic factors will propagate in the f_r calculation. In this study, the mean ε_k values were 7.3 ‰ for ^{18}O and 6.8 ‰ for ^{2}H. These values are lower than the default lake parameterizations (14.2 ‰ for ^{18}O and 12.5 ‰

Table 2. Recycled moisture fractions calculated based on the two-component mixing method, using *d*-excess in evaporation (d_E) and *d*-excess in water vapour at cloud base (d_{PV}, i.e. d_{adv} and d_{down}) as inputs.

	Liyang d_{PV} (‰)	Dongshan d_{PV} (‰)	d_E (‰)	f_r
WM1	22.7 ± 1.1*	25.0 ± 1.1	27.4 ± 2.1	0.48 ± 0.13
SM	13.9 ± 1.1	12.5 ± 1.1*	32.3 ± 2.1	0.07 ± 0.03
WM2	20.7 ± 1.1*	24.7 ± 1.1	31.4 ± 2.1	0.38 ± 0.05

Note: The superscript * indicates value of the upwind site.

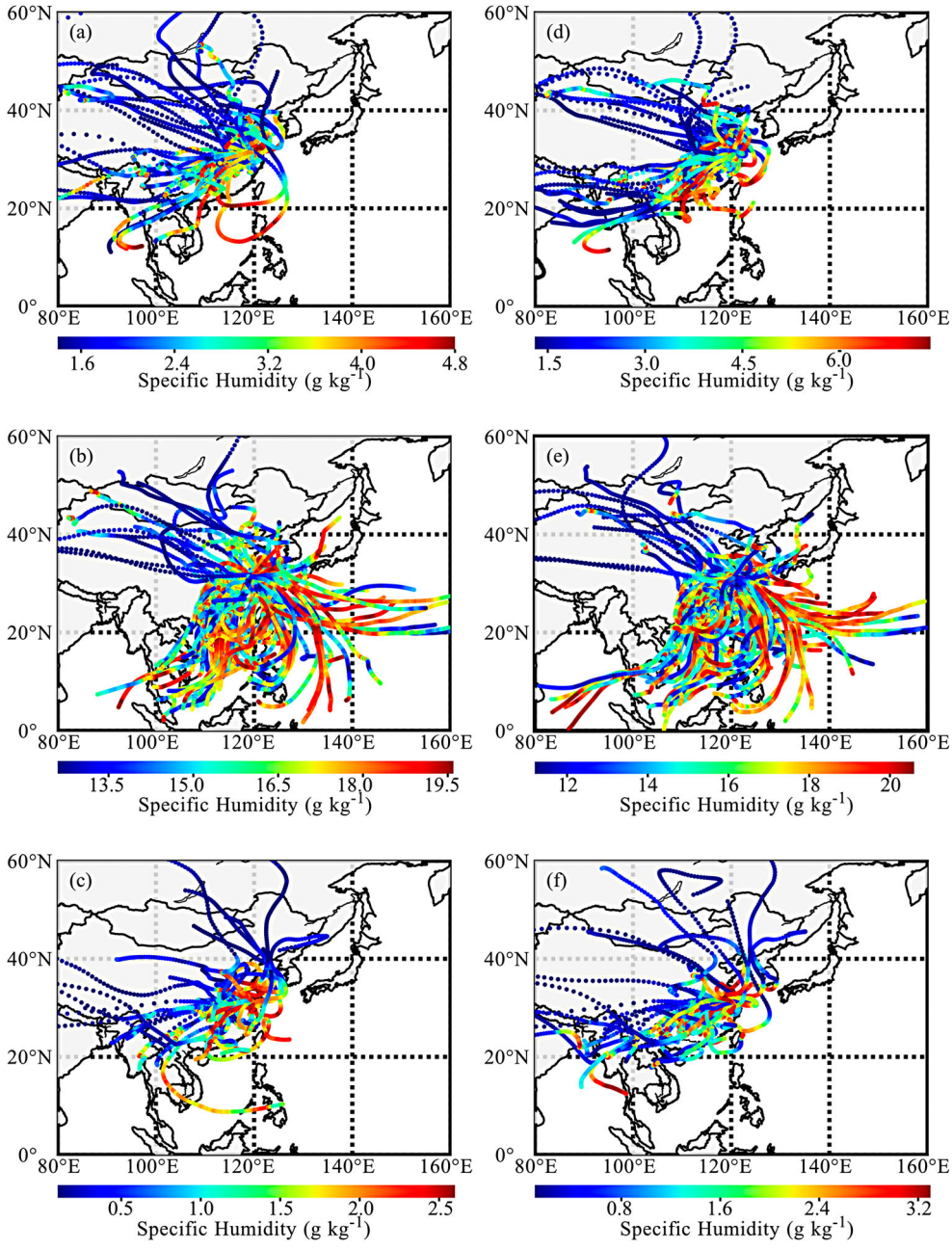

Figure 5. Specific humidity along the back trajectories during the first winter monsoon period (a and d), summer monsoon period (b and e) and the second winter monsoon period (c and f) at Liyang (left panels) and Dongshan (right panels).

for ^{2}H) used in many lake isotopic studies. Xiao et al. [29] found that the oceanic values are in good agreement with the kinetic factors determined experimentally using the gradient diffusion method for Lake Taihu. If the default lake ε_k values were used, d_E would increase to 70.1, 75.3 and 74.4 ‰, for the three monsoon periods, respectively, which

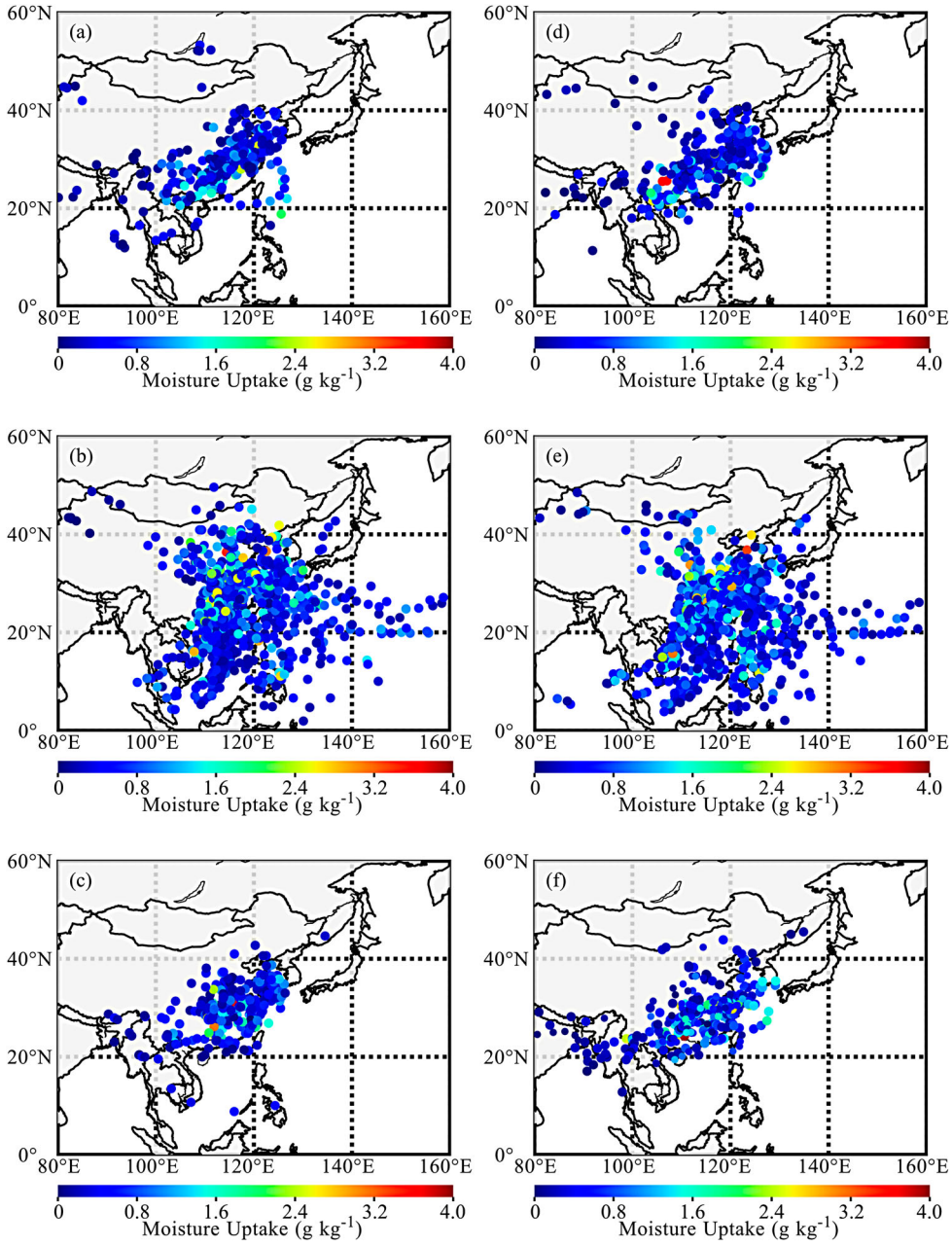

Figure 6. Moisture uptake along the back trajectories during the first winter monsoon period (a and d), summer monsoon period (b and e) and the second winter monsoon period (c and f) at Liyang (left panels) and Dongshan (right panels).

is 42.7–43.0 ‰ higher than the results obtained from the oceanic parameterization ε_k values (Table 2). The corresponding f_r values would be 0.05 ± 0.01, 0.02 ± 0.01 and 0.07 ± 0.01 for the three monsoon periods, respectively. The difference between summer and winter monsoons would become much smaller than shown in Table 2.

Similarly, the recycling rate calculation for the Great Lakes was also shown to be sensitive to the kinetic factor, decreasing from 0.17 with the oceanic parameterization to 0.07 with the default lake parameterization [26].

In the sub-cloud evaporation process, the raindrop *d*-excess becomes lower than its initial in-cloud value [31–34]. At Lake Taihu, the influence of sub-cloud evaporation on d_P was comparable between the two sites (Table 1). In other words, the spatial variation in d_{PV} ($d_{down} - d_{adv}$ in Equation (1)) was not sensitive to the effect of sub-cloud evaporation (Table 1). If the sub-cloud evaporation was not corrected, the difference between *d*-excess in evaporation and advection airmass ($d_E - d_{adv}$ in Equation (1)) would increase slightly from 1.2–2.2 ‰, and f_r would decrease to 0.43 ± 0.08, 0.05 ± 0.02 and 0.25 ± 0.04 for the three monsoon periods, respectively. In a related study, Froehlich et al. [25] reported that the sub-cloud evaporation influence would cause a low bias in the moisture recycling fraction in the Alpine region of Austria by 0–30%.

The changes in the recycling fraction caused by sub-cloud evaporation (0.02–0.13) are smaller than the changes due to the choice of the kinetic factor of surface evaporation (0.05–0.43). One reason is that sub-cloud evaporation is weak (about 4% at our two sites; Figure 3) in the humid sub-tropical monsoon climate [31,32]. The effect of sub-cloud evaporation on the calculation of recycled moisture would be larger at semi-arid or arid sites.

4.2. Comparison with published recycling fractions

Using a two-component mixing model, Peng et al. [62] estimated that the recycling fraction is 0.11 ± 0.07 during the summer monsoon for Eastern China, which contains our study region. Yuan et al. [63] reported a recycling fraction of 0.09 ± 0.02 for the same time and region from a regional climate model simulation. Their estimates are comparable to our summer result.

Previous studies on moisture recycling have been conducted for the Great Lakes in temperate climate [1,2,4,10,31] and Qinghai Lake in plateau climate [3]. These studies all use the two-component mixing model with the Craig–Gordon parameterization for the lake isotopic compositions. Corcoran et al. [4] found that f_r for the Laurentian Great Lakes is 0.09 in the summer and 0.12 in the winter. Other authors have reported f_r in the range of 0.04–0.16 during the summer months [1,9,10]. Cui and Li [3] reported that f_r for Qinghai Lake on the Tibetan Plateau value is 0.15, 0.26 and 0.23 for the spring, summer and autumn, respectively. Our summer f_r value is within the range of the values reported in these studies, but our winter f_r is larger.

4.3. The seasonal variability of moisture recycling at Lake Taihu region

Similar seasonal variability of moisture recycling, i.e. higher f_r in the winter and lower f_r in the summer, has been reported for the Great Lakes [4] and for monsoon regions [23,41,42]. For the Great Lakes, Corcoran et al. [4] attributed the seasonal variability of moisture recycling to the seasonal variability of lake evaporation at the Great Lakes where the maximum evaporation occurs in the cold season [64,65]. At Lake Taihu, the maximum monthly evaporation occurs in the summer: The evaporation rate during the summer monsoon months was about five times that during the winter monsoon

[14,39,40]. So lake evaporation seasonality cannot explain the seasonal variability of the moisture recycling fraction. Since large scale advection and local moisture recycling are the two sources of precipitation [17], an alternative explanation is that difference of the advected air conditions, e.g. specific humidity. Like other monsoon sites [18,37,38], the lower background moisture in the winter monsoon periods than that in the summer monsoon period, but comparable amount of uptake caused by the seasonality of moisture source is responsible for the seasonal variability of f_r at Lake Taihu.

5. Summary

At Liyang and Dongshan, δ^2H_P, $\delta^{18}O_P$ and d_P showed spatial variability consistent with lake evaporation influence. The d_P was higher at the downwind site and lower at the upwind site of the lake, indicating the lake evaporation contribution to precipitation. The magnitude of spatial variation of d_P in the summer monsoon period (1.1 ‰) was smaller than that in the winter monsoon periods (3.0 and 2.9 ‰ for each). After sub-cloud evaporation calibration, the spatial variation in d_P was 2.3, 1.4 and 3.2 ‰ for the first winter monsoon period, the summer monsoon period and the second winter monsoon period, respectively. Calculated from the Craig–Gordon model, d_P were 27.4, 32.3 and 31.4 ‰ for the three monsoon periods, respectively.

For the first winter monsoon period, the summer monsoon period and the second winter monsoon period, the recycled moisture fractions were 0.48 ± 0.13, 0.07 ± 0.03 and 0.38 ± 0.05, respectively. At the Lake Taihu region, if the lake parameterization kinetic fractionation factors were used, f_r values would decrease to 0.05 ± 0.01, 0.02 ± 0.01 and 0.07 ± 0.01 for the three monsoon periods, respectively. If the sub-cloud evaporation was not corrected, f_r would be 0.43 ± 0.08, 0.05 ± 0.02 and 0.25 ± 0.04 for the three monsoon periods, respectively. The seasonal variability of moisture recycling was attributed to differences in the specific humidity of the advected air.

Acknowledgements

The authors would like to thank all the participants of the experiments.

Disclosure statement

No potential conflict of interest was reported by the author(s).

Funding

This work got support from the National Natural Science Foundation of China [grant numbers 41975143 and 42021004], the National Key Research & Development Program of China [grant numbers 2020YFA0607501 and 2019YFA0607202], the China Scholarship Council, and the Key Laboratory of Meteorology and Ecological Environment of Hebei Province [grant number Z201901H].

ORCID

Yongbo Hu http://orcid.org/0000-0002-4752-4798

References

[1] Gat JR, Bowser CJ, Kendall C. The contribution of evaporation from the Great Lakes to the continental atmosphere: estimate based on stable isotope data. Geophys Res Lett. 1994;21:557–560.

[2] Scott RW, Huff FA. Impacts of the Great Lakes on regional climate conditions. J Great Lakes Res. 1996;22:845–863.

[3] Cui BL, Li XY. Stable isotopes reveal sources of precipitation in the Qinghai Lake basin of the northeastern Tibetan Plateau. Sci Total Environ. 2015;527–528:26–37.

[4] Corcoran MC, Thomas EK, Boutt DF. Event-based precipitation isotopes in the Laurentian Great Lakes region reveal spatiotemporal patterns in moisture recycling. J Geophys Res Atmos. 2019;124:5463–5478.

[5] Seneviratne SI, Lüthi D, Litschi M, et al. Land–atmosphere coupling and climate change in Europe. Nature. 2006;443:205–209.

[6] Zhou S, Park Williams A, Berg AM, et al. Land–atmosphere feedbacks exacerbate concurrent soil drought and atmospheric aridity. Proc Natl Acad Sci USA. 2019;116:18848–18853.

[7] Koster RD, Guo Z, Bonan G, et al. Regions of strong coupling between soil moisture and precipitation. Science. 2004;305:1138–1140.

[8] Baker JCA, Garcia-Carreras L, Buermann W, et al. Robust Amazon precipitation projections in climate models that capture realistic land–atmosphere interactions. Environ Res Lett. 2021;16:074002.

[9] Machavaram MV, Krishnamurthy RV. Earth surface evaporative process: a case study from the Great Lakes region of the United States based on deuterium excess in precipitation. Geochim Cosmochim Acta. 1995;59:4279–4283.

[10] Bowen GJ, Kennedy CD, Henne PD, et al. Footprint of recycled water subsidies downwind of Lake Michigan. Ecosphere. 2012;3:1–16.

[11] Bryan AM, Steiner AL, Posselt DJ. Regional modeling of surface–atmosphere interactions and their impact on Great Lakes hydroclimate. J Geophys Res. 2015;120:1044–1064.

[12] Lehner B, Döll P. Development and validation of a global database of lakes, reservoirs and wetlands. J Hydrol. 2004;296:1–22.

[13] Wang Y, Gao Y, Qin H, et al. Spatiotemporal characteristics of lake breezes over Lake Taihu, China. J Appl Meteorol Climatol. 2017;56:2053–2065.

[14] Wang W, Xiao W, Cao C, et al. Temporal and spatial variations in radiation and energy balance across a large freshwater lake in China. J Hydrol. 2014;511:811–824.

[15] Wang W, Lee X, Xiao W, et al. Global lake evaporation accelerated by changes in surface energy allocation in a warmer climate. Nat Geosci. 2018;11:410–414.

[16] Brubaker KL, Entekhabi D, Eagleson PS. Estimation of continental precipitation recycling. J Clim. 1993;6:1077–1089.

[17] Trenberth KE. Atmospheric moisture recycling: role of advection and local evaporation. J Clim. 1999;12:1368–1381.

[18] Curio J, Maussion F, Scherer D. A 12-year high-resolution climatology of atmospheric water transport over the Tibetan Plateau. Earth Syst Dyn. 2015;6:109–124.

[19] Joussaume S, Jouzel J, Sadourny R. A general circulation model of water isotope cycles in the atmosphere. Nature. 1984;311:24–29.

[20] O'Connor JC, Santos MJ, Dekker SC, et al. Atmospheric moisture contribution to the growing season in the Amazon arc of deforestation. Environ Res Lett. 2021;16:084026.

[21] Peng H, Mayer B, Norman A-L, et al. Modelling of hydrogen and oxygen isotope compositions for local precipitation. Tellus B Chem Phys Meteorol. 2005;57:273–282.

[22] Griffis TJ, Wood JD, Baker JM, et al. Investigating the source, transport, and isotope composition of water vapor in the planetary boundary layer. Atmos Chem Phys. 2016;16:5139–5157.

[23] Gimeno L, Stohl A, Trigo RM, et al. Oceanic and terrestrial sources of continental precipitation. Rev Geophys. 2012;50:RG4003.

[24] Galewsky J, Steen-Larsen HC, Field RD, et al. Stable isotopes in atmospheric water vapor and applications to the hydrologic cycle. Rev Geophys. 2016;54:809–865.

[25] Froehlich K, Kralik M, Papesch W, et al. Deuterium excess in precipitation of alpine regions – moisture recycling. Isot Environ Health Stud. 2008;44:61–70.
[26] Xiao W, Qian Y, Lee X, et al. Hydrologic implications of the isotopic kinetic fractionation of open-water evaporation. Sci China Earth Sci. 2018;61:1523–1532.
[27] Craig H, Gordon LI. Deuterium and oxygen 18 variations in the ocean and the marine atmosphere. In: Tongiorgi E, editor. Stable isotopes in oceanographic studies and paleotemperatures. Pisa: Consiglio nazionale delle richerche, Laboratorio de geologia nucleare; 1965. p. 9–72.
[28] Horita J, Rozanski K, Cohen S. Isotope effects in the evaporation of water: a status report of the Craig–Gordon model. Isot Environ Health Stud. 2008;44:23–49.
[29] Xiao W, Lee X, Hu Y, et al. An experimental investigation of kinetic fractionation of open-water evaporation over a large lake. J Geophys Res Atmos. 2017;122:11,651–11,663.
[30] Xie C, Xiao W, Zhang M, et al. Isotopic kinetic fractionation of evaporation from small water bodies. J Hydrol. 2021;603:126974.
[31] Salamalikis V, Argiriou AA, Dotsika E. Isotopic modeling of the sub-cloud evaporation effect in precipitation. Sci Total Environ. 2016;544:1059–1072.
[32] Wang S, Zhang M, Che Y, et al. Influence of below-cloud evaporation on deuterium excess in precipitation of arid Central Asia and its meteorological controls. J Hydrometeorol. 2016;17:1973–1984.
[33] Putman AL, Fiorella RP, Bowen GJ, et al. A global perspective on local meteoric water lines: meta-analytic insight into fundamental controls and practical constraints. Water Resour Res. 2019;55:6896–6910.
[34] Wang S, Jiao R, Zhang M, et al. Changes in below-cloud evaporation affect precipitation isotopes during five decades of warming across China. J Geophys Res Atmos. 2021;126: e2020JD033075.
[35] Wang S, Zhang M, Che Y, et al. Contribution of recycled moisture to precipitation in oases of arid Central Asia: a stable isotope approach. Water Resour Res. 2016;52:3246–3257.
[36] Kerandi N, Arnault J, Laux P, et al. Joint atmospheric–terrestrial water balances for east Africa: a WRF-Hydro case study for the upper Tana River basin. Theor Appl Climatol. 2018;131:1337–1355.
[37] Jiao Y, Liu C, Liu Z, et al. Impacts of moisture sources on the temporal and spatial heterogeneity of monsoon precipitation isotopic altitude effects. J Hydrol. 2020;583:124576.
[38] Ma Q, Zhang M, Wang L, et al. Quantification of moisture recycling in the river basins of China and its controlling factors. Environ Earth Sci. 2019;78:392.
[39] Hu C, Wang Y, Wang W, et al. Trends in evaporation of a large subtropical lake. Theor Appl Climatol. 2017;129:159–170.
[40] Xiao W, Zhang Z, Wang W, et al. Radiation controls the interannual variability of evaporation of a subtropical lake. J Geophys Res Atmos. 2020;125:e2019JD031264.
[41] Tang Y, Pang H, Zhang W, et al. Effects of changes in moisture source and the upstream rainout on stable isotopes in precipitation – a case study in Nanjing, eastern China. Hydrol Earth Syst Sci. 2015;19:4293–4306.
[42] Li Y, An W, Pang H, et al. Variations of stable isotopic composition in atmospheric water vapor and their controlling factors – A 6-year continuous sampling study in Nanjing, eastern China. J Geophys Res Atmos. 2020;125:e2019JD031697.
[43] GNIP (Global Network of Isotopes in Precipitation). IAEA/GNIP precipitation sampling guide. Available from: http://www-naweb.iaea.org/napc/ih/documents/other/gnip_manual_v2.02_en_hq.pdf.
[44] Prechsl UE, Gilgen AK, Kahmen A, et al. Reliability and quality of water isotope data collected with a low-budget rain collector. Rapid Commun Mass Spectrom. 2014;28:879–885.
[45] Lee X, Liu S, Xiao W, et al. The Taihu Eddy flux network: an observational program on energy, water, and greenhouse gas fluxes of a large freshwater lake. Bull Am Meteorol Soc. 2014;95:1583–1594.
[46] Newman B, Tanweer A, Kurttas T. IAEA standard operating procedure for the liquid-water stable isotope analyser IAEA water resources programme. 2009. Available from: http://www-naweb.iaea.org/napc/ih/documents/other/laser_procedure_rev12.pdf.

[47] Deng B, Liu S, Xiao W, et al. Evaluation of the CLM4 lake model at a large and shallow freshwater lake. J Hydrometeorol. 2013;14:636–649.
[48] Zhang Z, Zhang M, Cao C, et al. A dataset of microclimate and radiation and energy fluxes from the Lake Taihu Eddy flux network. Earth Syst Sci Data. 2020;12:2635–2645.
[49] Kong Y, Pang Z, Froehlich K. Quantifying recycled moisture fraction in precipitation of an arid region using deuterium excess. Tellus Ser B–Chem Phys Meteorol. 2013;65:19251.
[50] Stewart MK. Stable isotope fractionation due to evaporation and isotopic exchange of falling waterdrops: applications to atmospheric processes and evaporation of lakes. J Geophys Res. 1975;80:1133–1146.
[51] Majoube M. Fractionnement en oxygène 18 et en deutérium entre l'eau et sa vapeur. J Chim Phys. 1971;68:1423–1436. French.
[52] Barnes SL. An empirical shortcut to the calculation of temperature and pressure at the lifted condensation level. J Appl Meteorol. 1968;7:511–511.
[53] Best AC. The size distribution of raindrops. Q J R Meteorol Soc. 1950;76:16–36.
[54] von Herrmann CF. Problems in meteorology. Mon Weather Rev. 1906;34:574–579.
[55] Best AC. Empirical formulae for the terminal velocity of water drops falling through the atmosphere. Q J R Meteorol Soc. 1950;76:302–311.
[56] Yakir D, Sternberg LDSL. The use of stable isotopes to study ecosystem gas exchange. Oecologia. 2000;123:297–311.
[57] Merlivat L, Jouzel J. Global climatic interpretation of the deuterium–oxygen 16 relationship for precipitation. J Geophys Res. 1979;84:5029–5033.
[58] Sodemann H, Schwierz C, Wernli H. Interannual variability of Greenland winter precipitation sources: Lagrangian moisture diagnostic and North Atlantic Oscillation influence. J Geophys Res Atmos. 2008;113:D03107.
[59] Breitenbach SFM, Adkins JF, Meyer H, et al. Strong influence of water vapor source dynamics on stable isotopes in precipitation observed in southern Meghalaya, NE India. Earth Planet Sci Lett. 2010;292:212–220.
[60] Wei Z, Lee X, Liu Z, et al. Influences of large-scale convection and moisture source on monthly precipitation isotope ratios observed in Thailand, Southeast Asia. Earth Planet Sci Lett. 2018;488:181–192.
[61] Wolf A, Roberts WHG, Ersek V, et al. Rainwater isotopes in central Vietnam controlled by two oceanic moisture sources and rainout effects. Sci Rep. 2020;10:16482.
[62] Peng P, Zhang XJ, Chen J. Modeling the contributions of oceanic moisture to summer precipitation in eastern China using ^{18}O. J Hydrol. 2020;581:124304.
[63] Yuan X, Xie Z, Zheng J, et al. Effects of water table dynamics on regional climate: a case study over east Asian monsoon area. J Geophys Res Atmos. 2008;113:D21112.
[64] Lofgren BM, Zhu Y. Surface energy fluxes on the Great Lakes based on satellite-observed surface temperatures 1992 to 1995. J Great Lakes Res. 2000;26:305–314.
[65] Blanken PD, Spence C, Hedstrom N, et al. Evaporation from Lake Superior: 1. Physical controls and processes. J Great Lakes Res. 2011;37:707–716.